Spin Hall Magnetoresistance Induced by a Nonequilibrium Proximity Effect

H. Nakayama,[1,2] M. Althammer,[3,4] Y.-T. Chen,[5] K. Uchida,[1,6] Y. Kajiwara,[1] D. Kikuchi,[1,7] T. Ohtani,[1] S. Geprägs,[3] M. Opel,[3] S. Takahashi,[1] R. Gross,[3,8] G. E. W. Bauer,[1,5,7,*] S. T. B. Goennenwein,[3,†] and E. Saitoh[1,7,9,10,‡]

[1]*Institute for Materials Research, Tohoku University, Sendai 980-8577, Japan*
[2]*Laboratory for Nanoelectronics and Spintronics, Research Institute of Electrical Communication, Tohoku University, Sendai 980-8577, Japan*
[3]*Walther-Meißner-Institut, Bayerische Akademie der Wissenschaften, 85748 Garching, Germany*
[4]*Center for Materials Information Technology MINT and Department of Chemistry, University of Alabama, Tuscaloosa, Alabama 35487, USA*
[5]*Kavli Institute of NanoScience, Delft University of Technology, 2628 CJ Delft, The Netherlands*
[6]*PRESTO, Japan Science and Technology Agency, Saitama 332-0012, Japan*
[7]*WPI Advanced Institute for Materials Research, Tohoku University, Sendai 980-8577, Japan*
[8]*Physik-Department, Technische Universität München, 85748 Garching, Germany*
[9]*CREST, Japan Science and Technology Agency, Tokyo 102-0076, Japan*
[10]*The Advanced Science Research Center, Japan Atomic Energy Agency, Tokai 319-1195, Japan*

(Received 31 October 2012; published 13 May 2013)

We report anisotropic magnetoresistance in Pt|$Y_3Fe_5O_{12}$ bilayers. In spite of $Y_3Fe_5O_{12}$ being a very good electrical insulator, the resistance of the Pt layer reflects its magnetization direction. The effect persists even when a Cu layer is inserted between Pt and $Y_3Fe_5O_{12}$, excluding the contribution of induced equilibrium magnetization at the interface. Instead, we show that the effect originates from concerted actions of the direct and inverse spin Hall effects and therefore call it "spin Hall magnetoresistance."

DOI: 10.1103/PhysRevLett.110.206601 PACS numbers: 72.25.Ba, 72.25.Mk, 75.47.−m, 75.76.+j

The resistance of a metallic magnet depends on its magnetization direction, a phenomenon called magnetoresistance (MR). Several types of MR, i.e., anisotropic magnetoresistance (AMR) [1], giant magnetoresistance [2–4], and tunnel magnetoresistance [5–9] are presently indispensable in data storage technology. For these MRs to occur, conduction electrons must pass through the magnet. Here we report the discovery of a fundamentally different MR that is caused by *nonequilibrium* proximity magnetization of a metallic Pt film attached to an electrically insulating magnet $Y_3Fe_5O_{12}$ (YIG). Although the conduction electrons in the Pt film cannot enter the magnetic insulator, the Pt|YIG bilayer resistance reflects the magnetization direction of insulating YIG.

Spin transport and charge transport phenomena are interconnected. For example, the spin Hall effect (SHE) refers to conversion of an electric current into a transverse spin current, i.e., a net flow of electron magnetic moments, due to the spin-orbit interaction (SOI). The conversion efficiency of the SHE is enhanced in heavy metals such as Pt in which the SOI is very strong [Fig. 1(a)]. The reciprocal of the SHE is the inverse spin Hall effect (ISHE), i.e., the conversion of an injected spin current into a transverse electric current or voltage [Fig. 1(c)]. Here the directions of electric-current flow $\mathbf{J}_e$, spin-current flow $\mathbf{J}_s$, and spin-current polarization $\boldsymbol{\sigma}$ are at right angles to one another [10–17].

The SHE generates spin currents and spin accumulations. On the other hand, the ISHE has become useful for detecting spin currents and spin-based electric power generation [10–17]. Here a question arises: Is it possible that SHE and ISHE operate simultaneously? Based on our recent understanding of interfacial spin mixing at the interface between a magnetic insulator and a metal [18–22], we can now answer this question affirmatively.

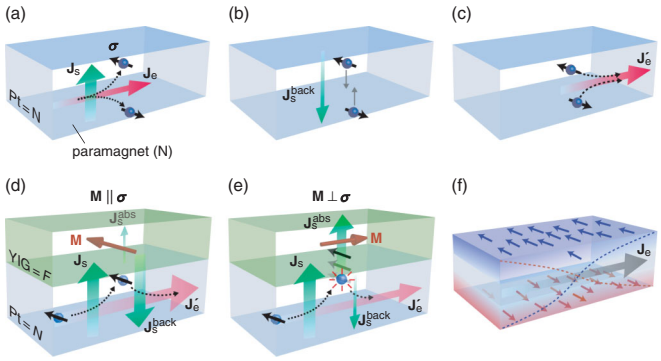

FIG. 1 (color). (a), (b), (c) Illustrations of the magnetic control of the conductivity due to the direct and inverse spin Hall effects (SHE and ISHE) in a paramagnetic thin film metal (N) with strong spin-orbit interaction attached to a ferromagnetic insulator (F). (d), (e) Illustrations of the geometric relation between the flow of electrons and accumulated spins in N = Pt and the magnetization in the magnetic insulator F = YIG. (f) Schematic illustration of the spin accumulation generated by nonequilibrium proximity due to the SHE in N. At the interfaces of N, the spin accumulation is formed depending on its spin polarization direction. Dashed curves in N show the electron motions with different spin polarization directions; the blue (red) arrows move to the upper (lower) side.

Consider a freestanding metallic thin film exhibiting strong SOI, e.g., Pt. An electric current along the film plane is applied to the Pt film. This $\mathbf{J}_e$ induces a spin current $\mathbf{J}_s$ due to the SHE in Pt that travels perpendicular to the film surface [10,13–15,23–26] with spin polarization $\boldsymbol{\sigma}$ parallel to the surface, as shown in Fig. 1(a). Second, at the film surface, the spin current is reflected back into the film [see Fig. 1(b)]. In real Pt films, this reflection is responsible for a nonequilibrium spin accumulation near the surface [Fig. 1(f)] and subsequent spin diffusion [27,28] as described below. Finally, the ISHE in Pt induces an electric current from the reflected spin current [see Fig. 1(c)], causing an electromotive force along the film plane. This additional electric current due to the combination of SHE and ISHE is always parallel to the original one; electric currents measured in a thin film with spin-orbit interaction inevitably include this additional contribution.

We may now control this process by putting an electrically insulating magnet, e.g., garnet-type YIG, on the Pt surface. This gives rise to interfacial spin mixing between YIG and Pt [18,19], i.e., to the spin-angular-momentum exchange between magnetization $\mathbf{M}$ in YIG and conduction-electron spin polarization $\boldsymbol{\sigma}$ in Pt. Spin-flip scattering is activated when $\boldsymbol{\sigma}$ and $\mathbf{M}$ are not collinear, as shown in Figs. 1(d) and 1(e). A part of the spin current is then absorbed by the magnetization as a spin-transfer torque [29–31] even at an interface to a magnetic insulator [21] and the spin-current reflection is suppressed. This absorption is maximized when $\mathbf{M}$ is perpendicular to $\boldsymbol{\sigma}$ and zero when $\mathbf{M}$ is parallel to $\boldsymbol{\sigma}$ [32]. Therefore, the conductivity enhancement due to SHE and ISHE is expected to be maximized (minimized) when $\mathbf{M}$ is perpendicular (parallel) to $\mathbf{J}_e$, because $\mathbf{J}_e$ is perpendicular to $\boldsymbol{\sigma}$. The Pt-film resistance is therefore affected by the magnetization direction in YIG, giving rise to the spin Hall magnetoresistance (SMR). Because the SMR in Pt is caused by nonequilibrium spin currents and appears only in the vicinity of the attached YIG on the scale of the spin diffusion length [28], Pt films with thicknesses on a comparable scale are necessary. We prepared a 12-nm-thick Pt film on a single-crystalline (111) YIG film [Fig. 2(a)]. YIG is a ferrimagnetic insulator with a large charge gap of ~2.7 eV [18,21]; its resistivity is larger than that of air, exceeding 10^{12} Ω cm. We measured the resistance R_{xx} of the Pt film at room temperature.

Figure 2(b) shows the observed resistance change $\Delta R_{xx}(H) = R_{xx}(H) - R_{xx}(H=0)$ in the Pt film as a function of the amplitude of the magnetic field H. In the experiment, the external magnetic field $\mathbf{H}$ was applied in the Pt film plane, perpendicular to the electric-current direction. In the present field range, the resistance of Pt depends on H only very weakly. However, as shown in Fig. 2(b), the Pt|YIG bilayer surprisingly exhibits a clear resistance change for $|\mathbf{H}| < 20$ Oe. The resistance decreases when increasing $|\mathbf{H}|$ from $H = 0$ with a small hysteresis. In contrast, outside this field range, viz.

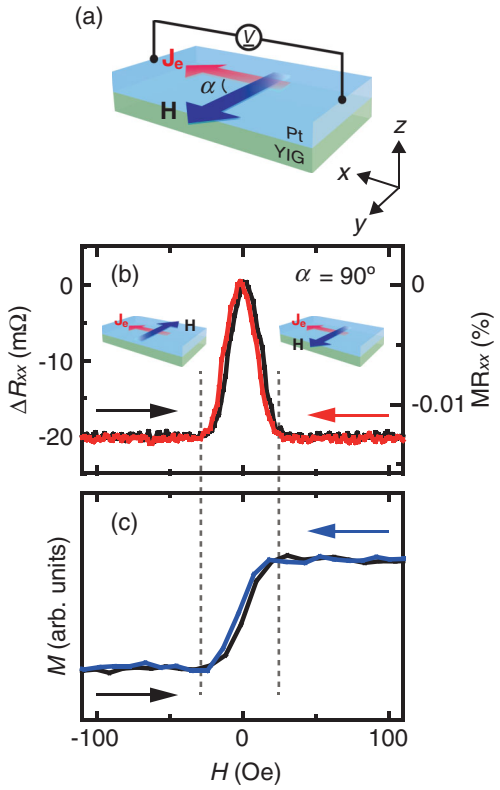

FIG. 2 (color). (a) Illustration of the experimental setup. The sample is a Pt|YIG bilayer film composed of a 1.3-μm-thick magnetic insulator YIG layer and a 12-nm-thick Pt layer. The electric resistance is measured by the four probe method. Here, $\mathbf{J}_e$, $\mathbf{H}$, and α represent the electric current in the Pt layer, the external magnetic field, and the relative in-plane angle between $\mathbf{J}_e$ and $\mathbf{H}$, respectively. (b) Magnetoresistance (MR) ΔR_{xx} for $\alpha = 90°$. (c) Magnetization M of a plain YIG film at 300 K.

$|\mathbf{H}| > 20$ Oe, the resistance is almost constant. The field range in which the resistance change appears coincides with the remagnetization process of the YIG layer such that $R_{xx}(H)$ has a maximum at the coercive fields of YIG. Figure 2(c) shows the H dependence of the in-plane magnetization of the YIG layer; the magnetization change is saturated for $|\mathbf{H}| > 20$ Oe, in agreement with the observed magnetoresistance. The diagonal component of the magnetoresistance $\mathrm{MR}_{xx} = \Delta R_{xx}(H)/R_{xx}(H=0)$ in the Pt film clearly reflects the remagnetization of the YIG film.

Because Pt is near the Stoner ferromagnetic instability, ferromagnetism induced in the Pt layer by the equilibrium proximity to YIG appears possible and could give rise to the AMR [33–36]. In fact, Pt atoms very close to the interface in Pt|Fe films are known to develop a finite magnetic moment due to a static proximity effect [34]. However, by systematic measurements on a number of reference structures, we are able to prove that such a proximity effect cannot be invoked to explain our observations in Pt|YIG. First, the SMR effect appears even when a 6-nm-thick Cu layer is inserted between the Pt and the

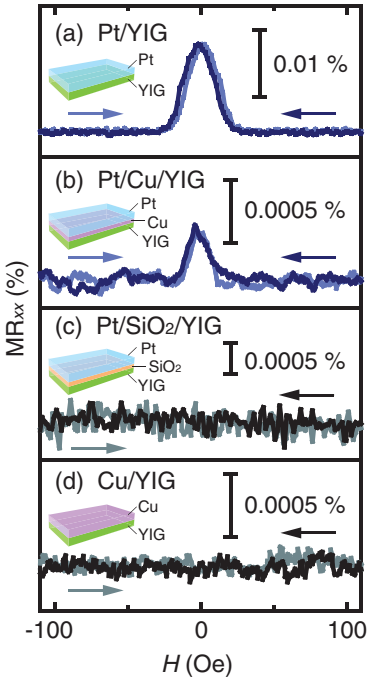

FIG. 3 (color). Control MR experiments on (a) Pt (12 nm)|YIG, (b) Pt (12 nm)|Cu (6 nm)|YIG, (c) Pt (12 nm)|SiO_2(6 nm)|YIG, and (d) Cu (6 nm)|YIG composite films, respectively. Here, the length and width of the Hall bars are 2.2 and 1.0 mm, respectively. The in-plane external magnetic field is applied perpendicular to the electric current, $\alpha = 90°$. The insets sketch the different samples.

YIG layers as shown in Fig. 3(b); Cu is very far from the Stoner instability and the nonlocal exchange force does not reach over such a thickness. Cu has a long (several hundred nanometers) spin diffusion length [27,28] and a very small SHE, viz. weak spin-orbit interaction, and carries a spin current over long distances. The observation of the MR_{xx} signal in Pt|Cu|YIG clearly shows that a magnetized Pt layer cannot explain the observed MR. The reduced MR ratio in Fig. 3(b) relative to Fig. 3(a) is caused by the short-circuit current path through the highly conductive Cu spacer [26]. Before sputtering the Pt layer of this sample, we confirmed that at least more than 95% of the YIG surface is covered with Cu film using energy dispersive x-ray analysis for the whole surface. For confirmation, we furthermore checked that the MR_{xx} signal disappears by replacing the Cu layer with an insulating SiO_2 layer as shown in Fig. 3(c), where SiO_2 is a nonmagnetic insulator allowing no spin current to pass. The MR_{xx} signal also disappears in a 6-nm-thick single layer Cu film on YIG [Fig. 3(d)] in which the spin-orbit interaction is very weak [18,19], indicating the crucial role of the spin-orbit interaction, or the SHE, while electromagnetic artifacts can also be excluded as origin of the MR. The results in Figs. 3(b)–3(d) clearly indicate that stray magnetic fields from the boundary of the YIG structure are irrelevant to the origin of the MR discussed here.

Finally, we found that the magnetoresistance in the present system exhibits a magnetic field orientation dependence that is very different from the AMR but consistent with the SMR scenario sketched above (cf. Fig. 4), confirming again the irrelevance of the AMR in a magnetized Pt layer. The AMR and SMR critically differ in their angle dependence: the AMR is governed by the angle of the applied current to the magnetization direction [1] α_{cM}, while the SMR depends on the angle of the spin accumulation induced by the current with the magnetization $\alpha_{\sigma\mathrm{M}}$. This difference becomes manifest when the magnetic field direction is swept from the direction parallel to the electric-current direction to the direction normal to the film surface [Fig. 4(k), $\alpha = 0$, $\gamma = +90° \rightarrow 0$]. During this field-direction scan, $\alpha_{\sigma\mathrm{M}}$ keeps constant while α_{cM} varies from 90° to 0, and according to the theory of the SMR, and in contrast to the AMR, the resistance should not change. This unusual behavior offers a key test of the SMR scenario. Figure 4(e) shows the MR_{xx} of a Pt|YIG sample measured with changing the field direction from $\gamma = -90° \rightarrow 290°$ at $\alpha = 0$ [see Fig. 4(k)]. Because the magnetic field intensity is fixed at 12 kOe, far above the magnetization saturation field (~1.7 kOe), the magnetization is always aligned with the external magnetic field direction. Clearly, the ΔR_{xx} signal disappears in this magnetic field orientation scan, in striking contrast to the other field-direction scans [cf. Figs. 4(c)–4(f)]. This behavior is observed not only in the present sample (sample 1) but also universally in our qualitatively different Pt|YIG samples as exemplified for sample 2 [26] in Fig. 4(i). The disappearance of ΔR_{xx} is a unique feature of the SMR and cannot be explained by the AMR. We thus conclude that the AMR of a conventional, equilibrium proximity spin polarization in Pt can be ruled out as an explanation for the magnetoresistance observed in experiment.

We introduced the SMR in a simple ballistic picture of spin currents reflected at the interfaces. For quantitative modeling it is necessary to invoke the diffusive nature of transport as well as spin dissipation in the metallic film. Considering a thin Pt film in the xy plane with an electric current applied along the x direction, the SHE generates a spin current flowing in the z direction with the spin polarization along the y direction, thereby building up spin accumulations at the Pt|YIG and vacuum|Pt interfaces. Their gradients induce diffusive counter spin currents such that the total (net) spin current is continuous at the Pt|YIG interface and vanishes at the vacuum|Pt surface. The interface spin current depends on the relative direction of the magnetization with respect to the spin accumulation direction according to $(G_r/e)\mathbf{m} \times (\mathbf{m} \times \boldsymbol{\mu}_s)$, where G_r is the interface spin-mixing conductance, $\mathbf{m}$ is the magnetization direction, and $\boldsymbol{\mu}_s$ is the spin accumulation vector at the interface [32]. When $\mathbf{m} || \boldsymbol{\mu}_s$, the interface spin current vanishes (just as at the vacuum interface). However, when the magnetization is rotated by 90° (to any perpendicular direction), the accumulated spins are partially absorbed

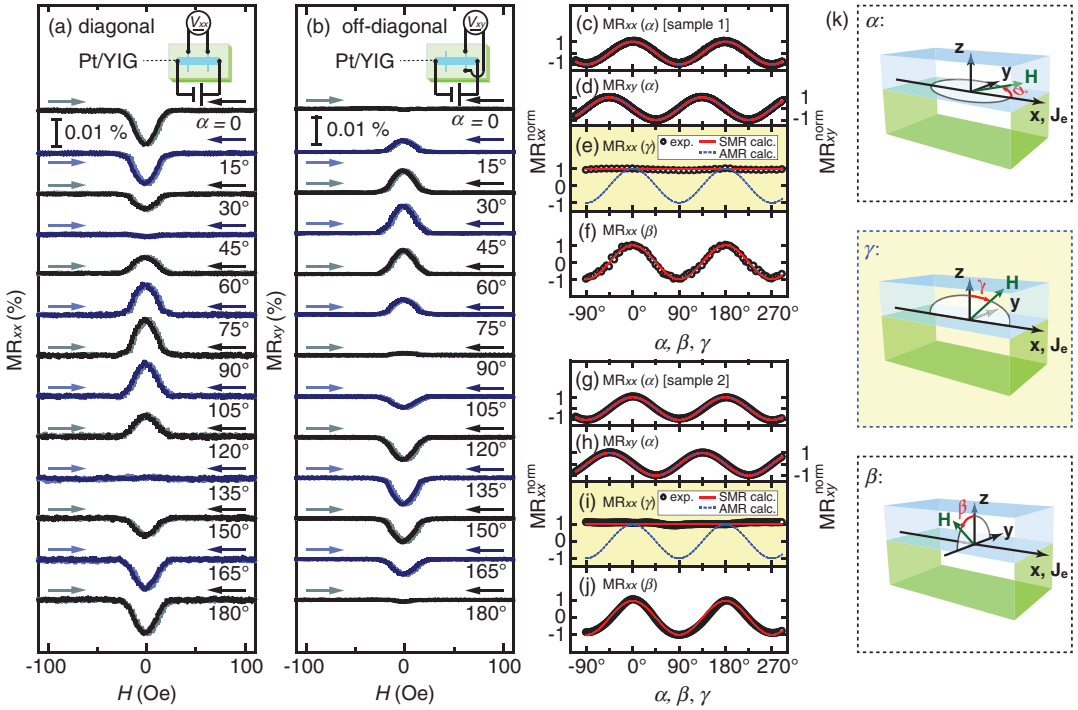

FIG. 4 (color). (a), (b) Diagonal and off-diagonal components of the MR in Pt|YIG films as a function of in-plane angle α. (c), (d), (e), (f), (g), (h), (i), (j) α, β, and γ dependence of the normalized MR_{xx} [$\mathrm{MR}_{xx}^{\mathrm{norm}} = \mathrm{MR}_{xx}/\mathrm{MR}_{xx}(\alpha = 0)$] and MR_{xy} [$\mathrm{MR}_{xy}^{\mathrm{norm}} = \mathrm{MR}_{xy}/\mathrm{MR}_{xy}(\alpha = -45°)$] in two different samples, where the angles α, β, and γ are defined in (k). The red and blue curves show MR expected according to the SMR model and the AMR model, respectively. (c) and (g) show α dependence of MR_{xx}, (d) and (h) show α dependence of MR_{xy}, (e) and (i) show γ dependence of MR_{xx}, and (f) and (j) show β dependence of MR_{xx}.

at the interface and dissipated as a spin-transfer torque to the magnetization, thereby modulating the spin-current distribution in Pt. Because the current-induced spin accumulation is polarized along the y direction, the polarization direction of the modulated spin current flowing along z varies as $\propto \mathbf{m} \times (\mathbf{m} \times \hat{\mathbf{y}})$. This in turn modulates the longitudinal (applied) electric current as $\propto \hat{\mathbf{y}} \cdot [\mathbf{m} \times (\mathbf{m} \times \hat{\mathbf{y}})] = m_y^2 - 1$ and induces a transverse electric current $\propto \hat{\mathbf{x}} \cdot [\mathbf{m} \times (\mathbf{m} \times \hat{\mathbf{y}})] = m_x m_y$ in the y direction due to the ISHE, where m_x and m_y are the Cartesian components of $\mathbf{m}$. The prefactors of these dependencies can be computed by spin diffusion theory [15] and quantum mechanical boundary conditions in terms of the spin-mixing conductance [32], thereby fully explaining the observed SMR in Pt|YIG [26]. The SMR resistivity change can hence be formulated as

$$\rho_{xx} = \rho_0 - \Delta\rho_{\mathrm{S}} m_y^2, \qquad \rho_{xy} = \Delta\rho_{\mathrm{S}} m_x m_y. \tag{1}$$

This is very different from the AMR phenomenology of polycrystalline conductive ferromagnets [1]

$$\rho_{xx} = \rho_\perp + \Delta\rho_{\mathrm{A}} m_x^2, \qquad \rho_{xy} = \Delta\rho_{\mathrm{A}} m_x m_y. \tag{2}$$

In both expressions the resistivity ρ_{xx} is measured along the direction of the electric-current flow $\mathbf{J}_e$ (along the x direction, cf. Fig. 4), while ρ_{xy} is the resistivity component recorded in the sample plane perpendicular to $\mathbf{J}_e$ (along the y direction), which typically appears in the magnetoresistive properties of ferromagnets [1]. ρ_0 is a constant resistivity offset, $\Delta\rho_{\mathrm{S}}$ and $\Delta\rho_{\mathrm{A}}$ ($= \rho_\parallel - \rho_\perp$) are the magnitude of the resistivity change as a function of the magnetization orientation, $\rho_\parallel$ and $\rho_\perp$ are the resistivities for magnetizations aligned along and perpendicular to $\mathbf{J}_e$, respectively. In Figs. 4(a) and 4(b), we show the evolution of the MR_{xx} and $\mathrm{MR}_{xy} = \rho_{xy}(H)/\rho_{xx}(H = 0)$ in sample 1 as a function of H, applied at different angles α. To quantitatively evaluate this dependence, we show the evolution of the MR_{xx} and MR_{xy} as a function of α in Figs. 4(c) and 4(d), respectively (symbols). The MR_{xx} for rotations of the magnetization in the plane perpendicular to the y direction (angle γ) and perpendicular to the x direction (angle β) are summarized in Figs. 4(e) and 4(f), while Figs. 4(i) and 4(j) show corresponding transport data for the sample 2. The behavior of the electric resistance expected from the AMR according to Eq. (2) is shown as blue curves in these panels, while the SMR predicted by Eq. (1) is depicted by red curves. The out-of-plane rotation data are consistently described in terms of the SMR; the angle-dependent MR data thus show that the MR observed in experiment indeed is due to the SMR effect. For a 12-nm-thick Pt film with the resistivity $8.6 \times 10^{-7}\ \Omega\,\mathrm{m}$ the theory sketched above agrees with the experimental

$\Delta\rho_S$ for the spin Hall angle $\theta_{SH} = 0.04$, the spin-flip diffusion length of $\lambda = 2.4$ nm, and the spin-mixing conductance [21] of $G_r = 5 \times 10^{14}\ \Omega^{-1}\,\mathrm{m}^{-2}$.

The SMR is a nonequilibrium proximity effect: the resistance of the metal film depends on the magnetic properties of the adjacent, electrically insulating ferromagnet. The SMR is not caused by a statically induced magnetization and is qualitatively different from conventional magnetoresistance effects, such as AMR, giant magnetoresistance, and tunnel magnetoresistance, where an electric current must flow through the magnetic layers. The SMR enables remote electrical sensing of the magnetization direction in a magnetic insulator. This also implies that the SMR makes the integration of insulating ferromagnets into electronic circuits possible, thereby avoiding current-induced deterioration of magnets due to, e.g., electromigration or heating. Finally, the SMR allows studying and quantifying spin Hall effects in paramagnetic metals as well as spin transfer to magnetic insulators via simple dc magnetoresistance measurements. We anticipate that SMR will develop into a standard technique in the nascent field of insulator spintronics.

The work at Tohoku University was supported by CREST-JST "Creation of Nanosystems with Novel Functions through Process Integration," Japan, PRESTO-JST "Phase Interfaces for Highly Efficient Energy Utilization," Japan, Grant-in-Aid for JSPS Fellows from JSPS, Japan, a Grant-in-Aid for Scientific Research A (24244051) from MEXT, Japan, a Grant-in-Aid for Scientific Research C (25400337) from MEXT, Japan, a Grant-in-Aid for Research Activity Start-up (24860003) from MEXT, Japan, LC-IMR of Tohoku University, and the Murata Science Foundation. The work at the Walther-Meißner-Institut and TU Delft was supported by the Deutsche Forschungsgemeinschaft (DFG) through priority programme SPP 1538 "Spin-Caloric Transport," project GO 944/4. G. E. W. B. acknowledges support from the Dutch FOM Foundation and EC-Project MACALO. H. N. and M. A. contributed equally to this work.

*g.e.w.bauer@imr.tohoku.ac.jp
†goennenwein@wmi.badw.de
‡saitoheiji@imr.tohoku.ac.jp

[1] T. R. McGuire and R. I. Potter, IEEE Trans. Magn. **11**, 1018 (1975).
[2] M. N. Baibich, J. M. Broto, A. Fert, F. N. Van Dau, F. Petroff, P. Etienne, G. Creuzet, A. Friederich, and J. Chazelas, Phys. Rev. Lett. **61**, 2472 (1988).
[3] G. Binasch, P. Grünberg, F. Saurenbach, and W. Zinn, Phys. Rev. B **39**, 4828 (1989).
[4] A. Fert, Rev. Mod. Phys. **80**, 1517 (2008).
[5] M. Julliere, Phys. Lett. **54A**, 225 (1975).
[6] T. Miyazaki and N. Tezuka, J. Magn. Magn. Mater. **139**, L231 (1995).
[7] J. S. Moodera, L. R. Kinder, T. M. Wong, and R. Meservey, Phys. Rev. Lett. **74**, 3273 (1995).
[8] S. Yuasa, T. Nagahama, A. Fukushima, Y. Suzuki, and K. Ando, Nat. Mater. **3**, 868 (2004).
[9] S. S. P. Parkin, C. Kaiser, A. Panchula, P. M. Rice, B. Hughes, M. Samant, and S.-H. Yang, Nat. Mater. **3**, 862 (2004).
[10] J. E. Hirsch, Phys. Rev. Lett. **83**, 1834 (1999).
[11] A. Azevedo, L. H. Vilela-Leão, R. L. Rodríguez-Suárez, A. B. Oliveira, and S. M. Rezende, J. Appl. Phys. **97**, 10C715 (2005).
[12] E. Saitoh, M. Ueda, H. Miyajima, and G. Tatara, Appl. Phys. Lett. **88**, 182509 (2006).
[13] S. O. Valenzuela and M. Tinkham, Nature (London) **442**, 176 (2006).
[14] T. Kimura, Y. Otani, T. Sato, S. Takahashi, and S. Maekawa, Phys. Rev. Lett. **98**, 156601 (2007).
[15] S. Takahashi and S. Maekawa, J. Phys. Soc. Jpn. **77**, 031009 (2008).
[16] O. Mosendz, J. E. Pearson, F. Y. Fradin, G. E. W. Bauer, S. D. Bader, and A. Hoffmann, Phys. Rev. Lett. **104**, 046601 (2010).
[17] A. Azevedo, L. H. Vilela-Leão, R. L. Rodríguez-Suárez, A. F. Lacerda Santos, and S. M. Rezende, Phys. Rev. B **83**, 144402 (2011).
[18] Y. Kajiwara *et al.*, Nature (London) **464**, 262 (2010).
[19] K. Uchida *et al.*, Nat. Mater. **9**, 894 (2010).
[20] B. Heinrich, C. Burrowes, E. Montoya, B. Kardasz, E. Girt, Y.-Y. Song, Y. Sun, and M. Wu, Phys. Rev. Lett. **107**, 066604 (2011).
[21] X. Jia, K. Liu, K. Xia, and G. E. W. Bauer, Europhys. Lett. **96**, 17 005 (2011).
[22] E. Padrón-Hernández, A. Azevedo, and S. M. Rezende, Phys. Rev. Lett. **107**, 197203 (2011).
[23] M. I. Dyakonov and V. I. Perel, Phys. Lett. **35A**, 459 (1971).
[24] Y. K. Kato, R. C. Myers, A. C. Gossard, and D. D. Awschalom, Science **306**, 1910 (2004).
[25] J. Wunderlich, B. Kaestner, J. Sinova, and T. Jungwirth, Phys. Rev. Lett. **94**, 047204 (2005).
[26] See Supplemental Material at http://link.aps.org/supplemental/10.1103/PhysRevLett.110.206601 for details on experimental methods, theory, and additional analysis.
[27] F. J. Jedema, A. T. Filip, and B. J. van Wees, Nature (London) **410**, 345 (2001).
[28] J. Bass and W. P. Pratt, Jr., J. Phys. Condens. Matter **19**, 183201 (2007).
[29] J. C. Slonczewski, J. Magn. Magn. Mater. **159**, L1 (1996).
[30] L. Berger, Phys. Rev. B **54**, 9353 (1996).
[31] D. C. Ralph and M. D. Stiles, J. Magn. Magn. Mater. **320**, 1190 (2008).
[32] A. Brataas, G. E. W. Bauer, and P. J. Kelly, Phys. Rep. **427**, 157 (2006).
[33] J. J. Hauser, Phys. Rev. **187**, 580 (1969).
[34] W. J. Antel, Jr., M. M. Schwickert, T. Lin, W. L. O'Brien, and G. R. Harp, Phys. Rev. B **60**, 12 933 (1999).
[35] M. Weiler *et al.*, Phys. Rev. Lett. **108**, 106602 (2012). (Including Supplemental Material).
[36] S. Y. Huang, X. Fan, D. Qu, Y. P. Chen, W. G. Wang, J. Wu, T. Y. Chen, J. Q. Xiao, and C. L. Chien, Phys. Rev. Lett. **109**, 107204 (2012).